Research Article Vol. 2, No. 5 / May 2015 / Optica 484

Experimental characterization of nonlocal photon fluids

David Vocke,[1,5] Thomas Roger,[1] Francesco Marino,[2] Ewan M. Wright,[1,3] Iacopo Carusotto,[4] Matteo Clerici,[1] and Daniele Faccio[1,*]

[1]Institute of Photonics and Quantum Sciences, Heriot-Watt University, Edinburgh EH14 4AS, UK
[2]CNR-INO, Largo Enrico Fermi 6, I-50025 Firenze, Italy
[3]College of Optical Sciences, University of Arizona, Tucson, Arizona 85721, USA
[4]INO-CNR BEC Center and Dipartimento di Fisica, Università di Trento, I-38123 Povo, Italy
[5]e-mail: dev1@hw.ac.uk
*Corresponding author: d.faccio@hw.ac.uk

Received 23 January 2015; revised 8 April 2015; accepted 17 April 2015 (Doc. ID 233144); published 14 May 2015

Quantum gases of atoms and exciton-polaritons are now well-established theoretical and experimental tools for fundamental studies of quantum many-body physics and suggest promising applications to quantum computing. Given their technological complexity, it is of paramount interest to devise other systems where such quantum many-body physics can be investigated at lesser technological expense. Here we examine a relatively well-known system of laser light propagating through thermo-optical defocusing media: based on a hydrodynamic description of light as a quantum fluid of interacting photons, we investigate such systems as a valid room-temperature alternative to atomic or exciton–polariton condensates for studies of many-body physics. First, we show that by using a technique traditionally used in oceanography it is possible to perform a direct measurement of the single-particle part of the dispersion relation of the elementary excitations on top of the photon fluid and to detect its global flow. Then, using a pump-and-probe setup, we investigate the dispersion of excitation modes of the fluid: for very long wavelengths, a sonic, dispersionless propagation is observed that we interpret as a signature of superfluid behavior. © 2015 Optical Society of America

OCIS codes: (190.4400) Nonlinear optics, materials; (190.3270) Kerr effect; (190.4870) Photothermal effects.

http://dx.doi.org/10.1364/OPTICA.2.000484

1. INTRODUCTION

Quantum gases, i.e., systems in which the thermal de Broglie wavelength is larger than the average particle distance, are an ever-increasingly important area of theoretical and experimental study, with applications as diverse as quantum computing and quantum simulation of general relativity models. The most important example of such physics is the Bose–Einstein condensate (BEC), in which a macroscopic number of bosonic particles at low temperature share the same wave function. After early work on liquid helium, the physics of condensates has been experimentally studied in ultracold atomic gases and, more recently, in exciton–polariton fluids in semiconductor microcavities. Building on these latter studies, an ever-growing community is now active on the study of the so-called quantum fluids of light, where the many-photons forming the beam are seen as a gas of interacting particles via the optical nonlinearity of the medium [1]. Among the many hydrodynamic effects that are presently being studied in such fluids of light, we can mention turbulence [2], where the general physical processes found in a fluid or superfluid can be found in many other systems, such as plasmas or in astrophysical systems. Another intriguing direction is so-called "analogue gravity," in which flowing fluids are used to model gravitational space–time geometries [3–6]. Waves propagating on top of a flowing medium behave the same way as light waves in a gravitational field. Hence, by tailoring the properties and flow geometry of such a medium, it is possible to mimic gravitational space–times in a laboratory experiment. As an alternative to actual flowing fluids, optical analogues obtained using laser beams propagating through nonlinear self-defocusing media or confined in nonlinear optical cavities have been proposed to create a photon fluid with the desired flow pattern. In these systems the fluid properties can be controlled through the phase and intensity of the incident optical field, as well as by the refractive index profile and the structural boundaries of the medium [7–9]. For example, a theoretical framework for photon fluids [1,7,8,10,11] has shown that sound-like excitations experience a curved space–time, and hence are promising models for analogue gravity experiments. A full quantum simulation showing evidence for analog Hawking radiation from a black hole horizon in a fluid of light was performed in [12] and the first experimental reports of black hole horizons in fluids of light were reported in [13,14]. The effective photon–photon interaction in the nonlinear

medium arises from the third-order Kerr nonlinearity [15], i.e., the local change in refractive index proportional to the light intensity $\Delta n = n_2|E|^2$: a defocusing nonlinearity with $n_2 < 0$ giving repulsive interactions is required to observe a dynamically stable photon fluid. Such a nonlinearity may be obtained through the thermo-optic effect, i.e., an intense laser beam locally heats the medium, which reacts by decreasing the refractive index proportionally to the deposited laser energy, thus giving rise to an effective repulsive photon–photon interaction [16].

Here we study and propose a relatively well-known nonlinear medium, i.e., the thermal defocusing medium described above, but revisited within the context of a fluid of light. The aim is to study the extent to which such systems can indeed represent a novel platform for studying, at room temperature, the properties of quantum gases with an emphasis on (but not limited to) the exciting perspective of reproducing superfluid behavior, phonon propagation according to the Bogoliubov dispersion, and particle generation from a black hole horizon and in an analogue gravity setup. In the propagating geometry considered here, the dynamics of the fluid takes place in the transverse plane (x, y) of a laser beam propagating through a bulk nonlinear medium, so that the propagation coordinate z plays the role of the time coordinate t [10,11]. Hence, by imaging the evolution of the beam profile along the z coordinate, it is possible to detect the spatiotemporal evolution of effective sound modes in the photon fluid (i.e., small oscillations on the transverse beam profile) and extract information on the dispersion relation of its elementary excitations. Using a technique inspired from oceanography, we obtain information on the high wave vector part of the dispersion where excitations have a single-particle nature and we detect the effect of global flow of the fluid. Then, a pump-and-probe technique is presented, in which the probe beam is used to create elementary excitations in the fluid generated by the pump. Information on the elementary excitation dispersion is obtained from the lateral shift of the interference pattern of pump and probe beams: signatures of the collective nature of the excitations and of the nonlocality of the photon–photon interactions are identified and discussed. An important result of this study is the experimental verification of the existence of a (phonon) wavelength regime in which, using the terminology introduced by Chiao and Boyce, photon superfluidity can be observed [15].

2. THEORETICAL MODEL

The propagation of a monochromatic laser beam with a vacuum optical wavelength λ in a self-defocusing medium can be described at steady state by the nonlinear Schrödinger equation (NLSE):

$$\partial_z E = \frac{i}{2k}\nabla^2 E - i\frac{kn_2}{n_0}|E|^2 E, \tag{1}$$

where z is the propagation direction, $k = 2\pi n_0/\lambda$ the optical wave vector, and n_0 is the linear refractive index of the medium. The Laplacian term $\nabla^2 E$ with respect to the transverse coordinates $\mathbf{r}(x, y)$ describes the linear diffraction of the laser beam, where the second, nonlinear, term proportional to n_2 refers to the optical Kerr nonlinearity, i.e., an intensity-dependent refractive index. In this work, we will always take $n_2 < 0$, that is, a self-defocusing nonlinearity, which guarantees transverse stability of the beams. By writing the field E in terms of its amplitude and phase $E = E_{\mathrm{bg}}\exp(i\phi)$, Eq. (1) can be rewritten as two differential equations [17]:

$$\partial_\tau \rho + \nabla(\rho \boldsymbol{v}) = 0, \tag{2}$$

$$\partial_\tau \psi + \frac{1}{2}v^2 + \frac{c^2 n_2}{n_0^3}\rho - \frac{c^2}{2\,k^2 n_0^2}\frac{\nabla^2\sqrt{\rho}}{\sqrt{\rho}} = 0, \tag{3}$$

formally identical to the density and phase equations of a 2D BEC, the temporal variable $\tau = zn_0/c$ being proportional to the propagation distance. The optical background intensity $|E_{\mathrm{bg}}|^2$ is identified as the photon fluid density ρ and the phase ϕ defines a fluid velocity $\boldsymbol{v} = (c/kn_0)\nabla\phi = \nabla\psi$.

The small amplitude perturbations $E = E_{\mathrm{bg}} + \epsilon$ (E_{bg} is the background field) can be described within the Bogoliubov theory in terms of sound waves on top of the photon fluid [10,18]. In the spatially homogeneous case where E_{bg} does not depend on the transverse coordinate $\mathbf{r}$, a sound mode of wave vector $\boldsymbol{K}$ and amplitude $\alpha_{\boldsymbol{K}}$ has a plane-wave form:

$$\epsilon = \alpha_{\boldsymbol{K}} u_{\boldsymbol{K}}\exp(-i\Omega\tau + i\boldsymbol{K}\boldsymbol{r}) + \alpha^*_{\boldsymbol{K}} v_{\boldsymbol{K}}\exp(i\Omega\tau - i\boldsymbol{K}\boldsymbol{r}), \tag{4}$$

and its angular frequency Ω (in the temporal τ variable) satisfies the dispersion relation

$$(\Omega - \boldsymbol{v}\boldsymbol{K})^2 = \frac{c^2 n_2|E_{\mathrm{bg}}|^2}{n_0^3}K^2 + \frac{c^2}{4k^2 n_0^2}K^4. \tag{5}$$

Here, c is the speed of light and v the background flow velocity. Using the terminology of hydrodynamics, we note that, for low frequencies, the dispersion of the sound modes has a sonic character $\Omega \propto K$, whereas for higher frequencies the second term dominates and the sound modes follow a single-particle quadratic dispersion $\Omega \propto K^2$. The separation between these two regimes defines a characteristic length $\xi = \lambda/2\sqrt{n_0|n_2||E_{\mathrm{bg}}|^2}$, usually called the *healing length* in the BEC literature [18]. As a result, only long-wavelength sound modes with $\Lambda \gg \xi$ follow a sonic dispersion with a constant sound speed $c_s = \sqrt{c^2|n_2||E_{\mathrm{bg}}|^2/n_0^3}$. This is of particular relevance, since only a linear dispersion guarantees superfluid behavior [10] and, in the context of analogue gravity, Lorentz invariance in the acoustic metric [7,19].

Translating these concepts into the language of optics [10], $K = \sqrt{K_x^2 + K_y^2}$ is the magnitude of the transverse wave vector of the light field and $\Omega = (c/n_0)\Delta K_z$ is related to the change Δk_z in the wave vector along the propagation axis. To experimentally access the low frequency modes, i.e., the $\Lambda \gg \xi$ regime, the light has to propagate in the nonlinear medium for at least one oscillation period T, so with $\Lambda = c_s T \gg \xi$, one arrives at a minimum propagation length given by $z_{\min} \approx cT/n_0 \gg \lambda/\Delta n$. We therefore see that, for a reasonable nonlinearity of $\Delta n = 10^{-4}$, long samples with at least 10–20 cm length are required to observe a full period of oscillation for the modes that lie in the linear part of the dispersion. In the next sections we show a technique that allows softening of this requirement on the sample length.

3. NONLOCAL MEDIA

A natural choice for the nonlinear material is therefore a liquid that exhibits a thermo-optic nonlinearity. The main advantage is that samples of the required dimensions can be easily built and that they are isotropic. In thermo-optical media, self-defocusing of the laser beam arises due to partial absorption of the beam,

which results in heating effects and, thus, to a decrease in the refractive index [20,21]. Thermal nonlinearity is usually highly nonlocal, i.e., the change in refractive index at any position depends not only on the local intensity, but also on surrounding field intensities [22,23]. This is a result of heat conduction inside the nonlinear medium and has a striking influence on the wave dynamics in nonlinear optics [24–26]. The medium response may be described by a response function $R(\mathbf{r}, z)$ so that Δn can be written as

$$\Delta n(\mathbf{r}, z) = \gamma \int R(\mathbf{r} - \mathbf{r}')I(\mathbf{r}')\mathrm{d}\mathbf{r}'\mathrm{d}z', \tag{6}$$

with γ being a normalization factor and I the field intensity. In general, R depends on the nonlocal process in the material and can be of different shapes. It is also important to note that, due to the long-range nature of thermal diffusion, R will also depend on the boundary conditions, e.g., on the shape and materials used for the cell containing the liquid [23]. For thermo-optical media, an isotropic exponential decay was proposed for $R(\mathbf{r}, z) = 1/(2\sigma_L)\exp(-\sqrt{r^2 + z^2}/\sigma_L)$, where the width of the response function σ_L defines the degree of nonlocality [23,27].

Straightforward extension of the Bogoliubov theory to nonlocal media leads to a modified Bogoliubov dispersion of the form [16,27]

$$(\Omega - \boldsymbol{v}\boldsymbol{K})^2 = \frac{c^2 n_2 |E_{\mathrm{bg}}|^2}{n_0^3}\hat{R}(K, n_0\Omega/c)K^2 + \frac{c^2}{4\ k^2 n_0^2}K^4, \tag{7}$$

where $\hat{R}$ is the 3D Fourier transform of the response function $R(r, z)$. It is easy to see that, well within the paraxial approximation $K/k, v/c \ll 1$, the rescaled Bogoliubov frequency $n_0\Omega/c \ll K$, so the main contribution to the nonlocality comes from the K dependence of $\hat{R}$, and we can simplify $\hat{R}(K, n_0\Omega/c) \simeq \hat{R}(K, 0) = 1/(1 + K^2\sigma_L^2)$ in Eq. (7).

Examples of the Bogoliubov dispersion in nonlocal media with different parameters are shown in Fig. 1. For very low wave vectors $K \ll 1/\xi, 1/\sigma_L$ the nonlinearity is responsible for the linear, sonic shape of the dispersion $\Omega \simeq c_s K$. At very large wave vectors $K \gg 1/\xi, 1/\sigma_L$, the dispersion recovers the quadratic single-particle dispersion $\Omega \propto K^2$. The effect of the nonlocality is most interesting for $\sigma_L \gg \xi$; in this case, there is a wide range of $1/\sigma_L < K < 1/\xi$ where the nonlocality suppresses the effectiveness of the nonlinearity and the dispersion is pushed toward the single-particle dispersion already at $K \simeq 1/\sigma_L \ll 1/\xi$. For a sufficiently small σ_L and a sufficiently fast decrease of R (faster than the one we are considering here, e.g., Gaussian), a ring of roton-like minima appears in the dispersion for finite K [16]. As a sonic shape of the dispersion of excitations is essential for gravitational or superfluid analogies to be rigorous, experimental studies in this direction require having control over the nonlinear and nonlocal properties of the material.

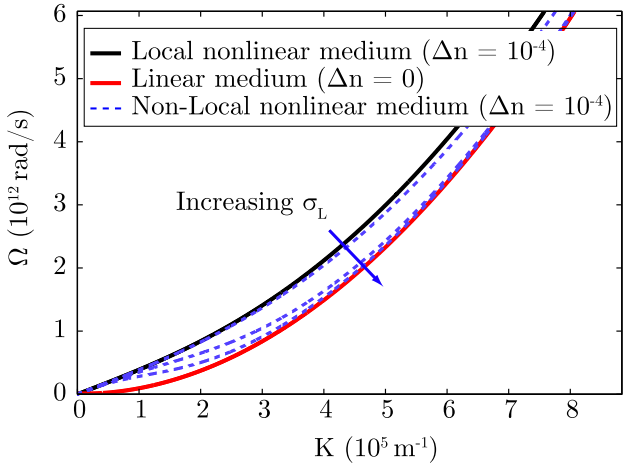

Fig. 1. Bogoliubov dispersion relation according to Eqs. (5) and (7). Local nonlinear media ($\Delta n = 10^{-4}$) show a linear part for wavelengths $\Lambda \gg \xi$ and $|\Delta n| > 0$ (black solid line, $\xi \sim 23$ μm, equivalent to $K = 2.7 \times 10^5$ 1/m). In nonlocal media, the effectiveness of the nonlinearity is suppressed for wavelengths $\Lambda < \sigma_L$ that result in a parabolic dispersion relation (the dashed blue lines correspond to a nonlocal nonlinear dispersion with $\sigma_L = 1$, 5 and 10 μm).

In the following, we report experimental evidence of a photon fluid in a nonlocal, self-defocusing medium. We adapted a method from oceanography to measure the spatiotemporal dispersion relation and show that by controlling the phase and intensity of the laser beam, we can imprint a flow as well as tune the velocity of acoustic waves. We then demonstrate a second method, based on tracking the sound speed of waves in the photon fluid as a function of input power, that allows us to measure both the local nonlinear refractive index change, Δn and the nonlocal length of the medium, σ_L.

4. EXPERIMENTAL RESULTS I: OCEANOGRAPHIC TECHNIQUE

The experiments (see Fig. 2 for a schematic layout) were carried out by launching a collimated CW laser beam with 532 nm wavelength through a cylindrical tube with length $L = 13$ cm (2 cm diameter) filled with a methanol/graphene solution with a refractive index $n_0 = 1.33$. The beam is magnified to a waist diameter of 1.6 cm by a $4f$ telescope, and the central portion with a radius of 1 cm is selected with an aperture to ensure a relatively flat intensity profile. Methanol is known to have a negative thermo-optic coefficient of $dn/dT \approx -4 \times 10^{-4}$ 1/K but has a very low absorption coefficient of $\alpha = 0.0006$ cm^{-1} [28]. Nanometric graphene flakes (7 nm average size) are therefore dissolved in the medium in order to increase absorption. Differently from widely used dyes, graphene does not exhibit any efficient fluorescence mechanism, so that most of the absorbed laser energy is converted directly into heat. By using a very dilute solution of graphene, it was possible to prepare samples with a total absorption that could be controllably chosen in the full 0 to ~100% region over the sample length and adjusted in our experiments so as to have 20% absorption. A camera/lens system is mounted on a computer-controlled longitudinal translation stage so that the transverse beam profile can be imaged at different positions along the propagation axis of the beam. The imaging was performed at a constant image distance to ensure uniform scaling in the transverse and z directions during scanning. Since the z axis maps into a time coordinate, it is possible to measure the spatiotemporal evolution of small intensity fluctuations on top of the beam by scanning along z and measuring the 2D beam profile at defined increments of Δz. The input beam diameter was large enough so that linear diffraction was negligible along the sample. To directly measure the dispersion relation, a technique adapted from oceanographic studies was used where surface waves that naturally occur were recorded in both space and time

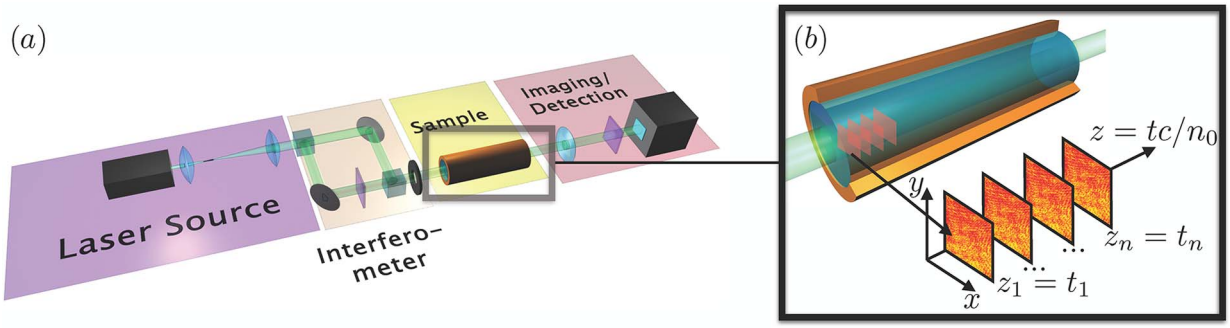

Fig. 2. (a) Experimental layout used for measuring the dispersion relation. A collimated, flat beam is launched through a cylindrical sample filled with a methanol/graphene solution and is imaged by a camera/lens system that can be translated along the propagation direction of the beam. (b) Detail of nonlinear sample showing example beam profiles at different propagation distances (i.e., equivalently for different propagation times) as measured in the experiment. An interferometer placed before the sample generates a pump and probe beam with a controllable relative angle (i.e., wavelength of the photon fluid excitations).

and by calculating the Fourier transform one obtains the dispersion of the medium [29–31].

In our experiment, the set of images is stored in a 3D (x, y, z) dataset: the origin of the observed fluctuations is due to (static) classical amplitude noise that is always present on the transverse profile of any laser beam (unless one invests significant effort to completely spatially filter it out). The dispersion $I(K_x, \Delta K_z)$ can be calculated via the Fourier transform of a lineout of the measured intensity signal $I(x, 0, z)$. The resulting spectrum can be converted to frequency using $\Omega = (c/n_0)\Delta K_z$. To enhance the signal-to-noise ratio, the data was averaged over 200 line-outs along the y direction. Examples of the measured dispersion of the photon fluid are shown in Figs. 3(a)–3(c). The spectra show some "folding," determined by the lattice of points at which the signal is sampled and then Fourier transformed. The large signal at $(K = 0, \Omega = 0)$ corresponds to the background pump beam. Some of the spectra also show vertical stripes or other features that do not lie on the dispersion curves and which we were able to attribute to small defects present, e.g., on the input or output window facets. The main finding of these measurements is the observation of an apparently purely parabolic dispersion for all spatial K-vectors and for all sets of parameters. Three different measurements are shown in Fig. 3 for three different angles of the input beam with respect to the sample (and imaging) axis in the x–z plane. This tilt angle creates a linear phase gradient along the tilt direction and, thus, according to the hydrodynamical equations [Eqs. (2) and (3)], controls the transverse flow of the photon fluid. This can clearly be seen in Figs. 3(b) and 3(c) for which the increasing input angles lead to increasing flow. The data is consistent with Eq. (5) with $\Delta n = 0$ and flow speeds $v_{bg} = 0$, 1.3×10^6 m/s, and 3.0×10^6 m/s [Figs. 3(a), 3(b), and 3(c), respectively]. We attribute the purely parabolic dispersion to the nonlocal nature of the material that, as discussed above, reduces the effectiveness of the nonlinearity for features smaller than the σ_L. A nonlocal length for methanol of $\sigma_L \approx 300$ μm has been reported [23], implying that only modes with a much smaller $K < 10^4$ m^{-1} would appear to have a linear dispersion (Fig. 1).

We emphasize that in these measurements we are imaging the various photon fluid planes inside the actual nonlinear medium. This may cause some issues related to the fact that we can no longer consider this a linear imaging measurement, and the nonlinearity may lead to deformations of the various object planes [32]. We did, however, experimentally verify that objects placed at the cell input could be imaged through the sample and that distortions appeared to be significant only in the presence of sharp transitions from very low to very high light intensity regions. We therefore expect that the images of the weak and smooth oscillations lying on top of the more intense laser beam background are not significantly distorted, and that the overall shape of the measured dispersion curve is indeed correct. This is corroborated by the fact that the dispersion relation [Eq. (5)] provides an excellent theoretical fit to the data for the zero-velocity flow case and provides a correct estimate of the photon fluid flow when the input beam is placed at an angle with respect to the imaging axis.

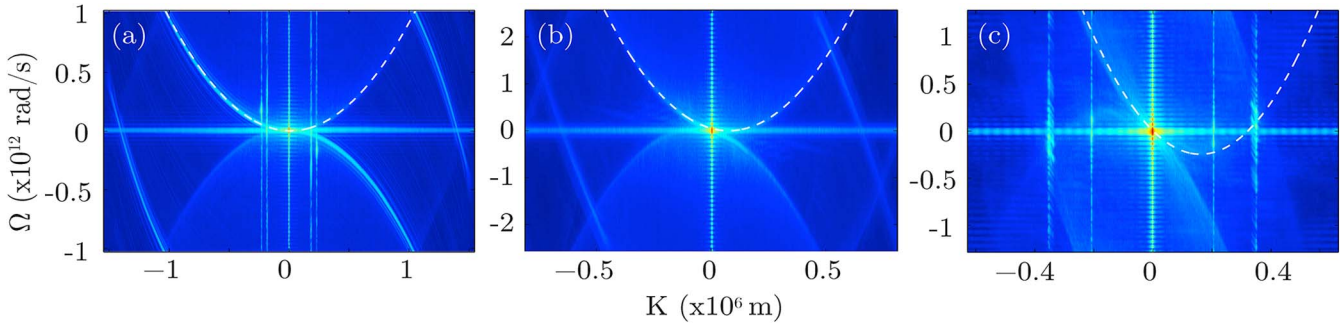

Fig. 3. Photon fluid dispersion relation with scanning distances of (a) 1.5 cm, (b) 5 cm, and (c) 12 cm. The flow v of the effective medium can be controlled by the phase of the background field: (a) $v_{bg} = 0$ m/s, (b) $v_{bg} = 1.3 \times 10^6$ m/s, and (c) $v_{bg} = 3.0 \times 10^6$ m/s.

However, it is clear that a more detailed and precise estimate of the low-frequency behavior and the presence or absence of superfluid behavior should be assessed by a technique that does not require imaging through the nonlinear medium. The results obtained with such a technique are discussed in the next section.

5. EXPERIMENTAL RESULTS II: PUMP-AND-PROBE TECHNIQUE

In this experiment, a pump–probe configuration was used to imprint a specific wavelength on top of the background beam, as proposed in [10]. We then study the wave dynamics for different background intensities. The probe beam was extracted from the pump beam using a beam splitter and was attenuated with a half-wave plate and a polarizing beam splitter. The probe beam was then recombined with the pump beam inside the sample: by controlling the relative angle of the two beams we created an interference pattern of the desired modulation depth (≈5%) and relative wave vector K. Both the pump and probe beams are loosely focused into the sample using a cylindrical lens pair to create an elliptical beam with a very wide major axis diameter of 1 cm and a minor axis diameter of 260 μm with a Rayleigh length ≈10 cm. The interference wave pattern (i.e., the photon fluid sound wave) is finally imaged at the output facet of the sample, and a shift of this pattern along the x direction can be measured as a function of the laser power [Fig. 4(a)]. The final imaging stage is performed with a 1-to-1 imaging $f =$ 300 mm lens. In the focal plane we place a mask to eliminate the four-wave mixed wave, thus suppressing interference between counterpropagating Bogoliubov modes and facilitating the measurement of the phase shift, so as to isolate the pump and probe beams. Our pump–probe setup is similar to that used in the past to study periodic soliton formation [33,34], albeit with a lower contrast in the pump–probe interference pattern, and, as we discuss below, our attention is focused on the dynamics of the photon-fluid sound waves.

As the beam propagates through the nonlinear medium, the phase velocity of the sound wave is determined by $v_P = \Omega/K$ with Ω given by Eq. (5) and hence is a function of the nonlinearity Δn. As the pump beam power is increased we therefore expect to observe a spatial shift of the sound wave pattern by ΔS due to the increase of the phase velocity. So, by using Eq. (7), we obtain an expression for $\Delta S = \Delta S(\Delta n, K)$:

$$\Delta S = \frac{K}{2k}\left[\sqrt{1+\frac{|\Delta n|}{n_0}\hat{R}(K)\left(\frac{2k}{K}\right)^2}-1\right]z. \tag{8}$$

By measuring ΔS for different values of the pump power we may therefore use Eq. (8) to estimate both Δn and σ_L. As a function of the sound wave vector K, one can recognize the finite limit $\Delta S \to \sqrt{\Delta n/n_0}$ determined by the speed of sound in the fluid of light. The local versus nonlocal nature of the nonlinearity is visible for short wavelengths. In the local case, the phase shift tends to 0 linearly in $1/K$ with a slope proportional to the refractive index change $|\Delta n|$. In the nonlocal case, an extra decay is introduced by the $\hat{R}(K)$ factor: for the case in which $\hat{R}(K) = 1/(1+(\sigma_L K)^2)$, for low K this tends to zero as K^{-2}. As a result, the phase shift tends to 0 much more quickly. While a nonzero ΔS is by itself a consequence of interactions, the nonlocal effect on the Bogoliubov dispersion is visible in the deviation of ΔS from a linear dependence on $1/K$.

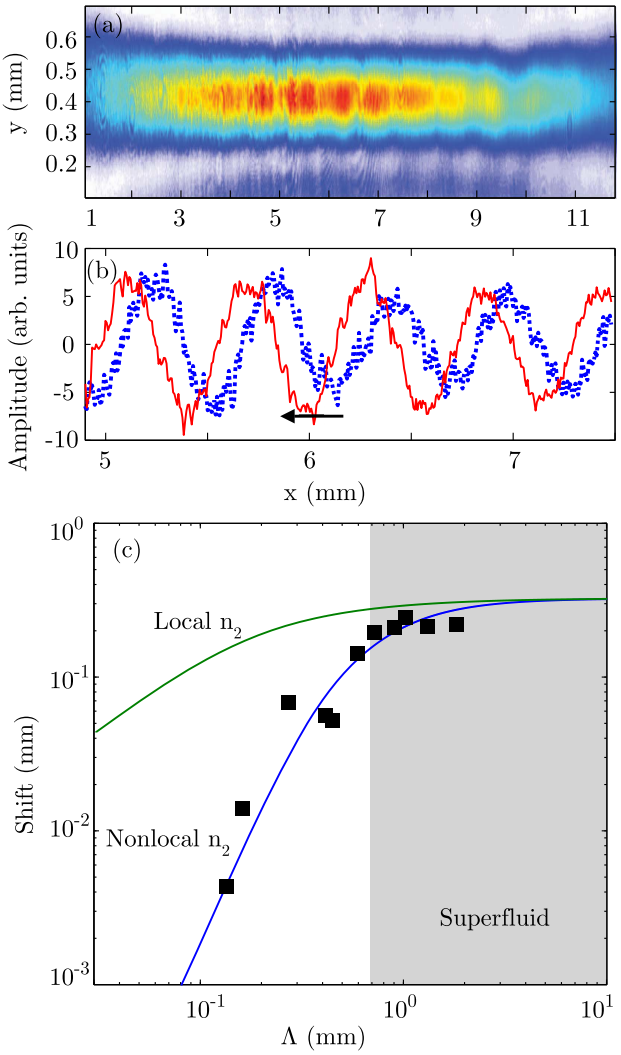

Fig. 4. (a) Raw data image of the beam at the sample output. The sound wave is barely visible due to the low (less than 10%) contrast of the amplitude modulation. (b) Amplitude profile of the sound wave after subtracting the pump beam profile for two different input pump powers: low-power measurement (dotted blue line) and high-power measurement (showing a shift in the wave, indicated by the arrow; solid red line). (c) Relative shift ΔS versus Λ: the solid green line shows the predicted shift for a local nonlinearity of $\Delta n = -7.6 \times 10^{-6}$; the corresponding healing length is $\zeta = 85$ μm. The solid blue line includes a nonlocal nonlinearity with $\Delta n = -7.6 \times 10^{-6}$ and nonlocal length $\sigma_L = 110$ μm. The shaded gray area ($\Lambda \gtrsim 10\zeta$) highlights the region in which, even in the presence of nonlocality, the medium acts as a superfluid. The black squares indicate the measured shift values at various wavelengths, several of which (i.e., for $\Lambda > 0.7$ mm) lie in the superfluid region.

The experimental data of the relative shifts of several transverse wavelengths $\Lambda = 2\pi/K$ between 120 μm and 1.8 mm at a fixed laser power of 28 mW (intensity, 1 W/cm^2) is shown in Fig. 4 (solid black squares). For comparison, the predicted shift in a medium with a purely local ($\hat{R} = 1$) nonlinearity ($\Delta n = -7.6 \times 10^{-6}$) according to Eq. (8) is also plotted (solid green line). In general, we found that it is not possible to obtain a satisfactory agreement with the experimental trend for any value of Δn and a purely local nonlinearity.

On the other hand, if we take into account the nonlocal factor $\hat{R}(K) = 1/(1+K^2\sigma_L^2)$ in Eq. (8), we obtain very good

agreement with the data with $\Delta n = -7.6 \times 10^{-6}$ and $\sigma_L = 110$ μm (solid blue line).

We note that the measurement of the phase shift is performed in the central region of the beam where the pump intensity can be considered as spatially uniform. Furthermore, to rule out alternative interpretations, such as deflection of the phonon waves by the broad intensity profile of the pump, we have experimentally checked that the wavelength of the sound wave does not vary during propagation through the nonlinear medium and does not show any position-dependent stretching effect.

A remarkable feature of these measurements is that for the longer wavelengths, i.e., for $\Lambda > 0.7$ mm, the observed shift appears to saturate and, within an 8% margin, is the same for all wavelengths. In other words, the phase velocity of the waves, $c_s = \Delta S/(Ln_0/c) = 3.8 \times 10^5$ m/s, does not depend on wavelength in this region (shaded in gray in the figure) and the dispersion relation is dominated by the linear behavior of the Bogoliubov term. This is a clear evidence of the linear dispersion of collective excitations typical of a superfluid or, in the language of general relativity, of Lorentz invariant propagation that is crucial for future analogue gravity experiments. Naturally, the observation of superfluid features in a system at room temperature is in itself of great interest, and future experiments will be directed at deepening our understanding and control over the flow and wave propagation in this nonlocal photon superfluid.

A crucial point here is that a standard Z-scan measurement would not be adequate for characterizing such a nonlocal nonlinearity. A Z-scan relies on translating the sample through the focus of a lens, i.e., through a region in which the transverse length scale of the beam is changing. The nonlinearity analyzed here shows a clear dependence on the transverse beam dimensions through the $\hat{R}$ response function. In a Z-scan measurement, the material would therefore respond with different effective nonlinearities at different measurement positions, resulting in a distorted Z-scan trace. We explicitly verified that this is indeed the case (data not shown).

6. CONCLUSIONS

We have reported a nonlinear optical experiment that aims at characterizing the physics of a photon fluid realized in a cavity-less nonlinear medium with a nonlocal optical nonlinearity of thermal origin. With a technique used in hydrodynamics, we measured the parabolic dispersion relation for small-amplitude small-wavelength noise excitations, and highlighted the evidence of a hydrodynamic flow in the presence of a linear phase term on the transverse beam profile. With a pump–probe technique we investigated the larger wavelength region by measuring the change in the phase velocity of collective excitations as a function of the pump intensity. In this way, we estimated the thermal nonlinearity to $\Delta n = -7.6 \times 10^{-6}$ and the nonlocal length $\sigma_L = 110$ μm. This measurement technique also highlighted one of the signatures of superfluid behavior of the photon fluid, i.e., a sonic, dispersionless propagation of its collective excitations. This result holds promise both for future room-temperature studies of superfluidity and for analogue gravity measurements that require a Lorentz invariant (i.e., dispersionless) flowing medium. Our measurements indicate that there is a readily attainable wavelength region in which such measurements may be feasible in the near future. However, the sound speed in the superfluid regime demonstrated is relatively low $c_s = 3.8 \times 10^5$ m/s and will require very long samples in order to observe significant wave propagation. Future work will therefore be directed at increasing the sound speed, e.g., by use of materials with higher nonlinearities. On the other hand, the degree of nonlocality can also be tuned by modifying the sample geometry [23] or absorption [35] and this opens opportunities for performing related experiments over a broader wavelength range.

Of course, the observation of a sonic, dispersionless propagation of collective excitations does not constitute a definitive proof of superfluidity. A crucial and natural demonstration of superfluidity will involve the study of the transition from laminar flow around an obstacle at subsonic flow speeds to turbulent dissipative flow with the formation of quantized vortices at supersonic flow speeds [10,36]. Furthermore, such media show promise for studies of hydrodynamical turbulence in the presence of nonlocal interactions and the study of collective dynamics of incoherent waves. Finally, extension of our experimental apparatus beyond the CW measurements shown here so as to measure also time-dependent fluctuations could provide access to quantum fluctuation features [11], such as analogue Hawking radiation [3].

Autonomous Province of Trento; Engineering and Physical Sciences Research Council (EPSRC) (EP/J00443X/1); European Research Council (ERC) (306559).

REFERENCES

1. I. Carusotto and C. Ciuti, "Quantum fluids of light," Rev. Mod. Phys. **85**, 299–366 (2013).
2. A. Picozzi, J. Garnier, T. Hanssom, P. Suret, S. Randoux, G. Millot, and D. N. Christodoulides, "Optical wave turbulence: towards a unified nonequilibrium thermodynamic formulation of statistical nonlinear optics," Phys. Rep. **542**, 1–132 (2014).
3. C. Barceló, S. Liberati, and M. Visser, "Analogue gravity," Living Rev. Relativity **14**, 3–159 (2011).
4. M. Novello, M. Visser, and G. E. Volovik, eds., *Artificial Black Holes* (World Scientific, 2002).
5. D. Faccio, F. Belgiorno, F. Cacciatori, V. Gorini, S. Liberati, and U. Moschella, eds., *Analogue Gravity Phenomenology* (Springer, 2013).
6. W. G. Unruh, "Experimental black-hole evaporation?" Phys. Rev. Lett. **46**, 1351–1353 (1981).
7. F. Marino, "Acoustic black holes in a two-dimensional photon fluid," Phys. Rev. A **78**, 063804 (2008).
8. F. Marino, M. Ciszak, and A. Ortolan, "Acoustic superradiance from optical vortices in self-defocusing cavities," Phys. Rev. A **80**, 065802 (2009).
9. I. Fouxon, O. V. Farberovich, S. Bar-Ad, and V. Fleurov, "Dynamics of fluctuations in an optical analogue of the Laval nozzle," Europhys. Lett. **92**, 14002 (2010).
10. I. Carusotto, "Superfluid light in bulk nonlinear media," Proc. R. Soc. A **470**, 20140320 (2014).
11. P.-É. Larré and I. Carusotto, "Propagation of a quantum fluid of light in a bulk nonlinear optical medium: general theory and response to a quantum quench," arXiv:1412.5405 (2015).
12. D. Gerace and I. Carusotto, "Analog Hawking radiation from an acoustic black hole in a flowing polariton superfluid," Phys. Rev. B **86**, 144505 (2012).
13. M. Elazar, V. Fleurov, and S. Bar-Ad, "All-optical event horizon in an optical analog of a Laval nozzle," Phys. Rev. A **86**, 063821 (2012).
14. H. S. Nguyen, D. Gerace, I. Carusotto, D. Sanvitto, E. Galopin, A. Lemaitre, I. Sagnes, J. Bloch, and A. Amo, "An acoustic black hole in a stationary hydrodynamic flow of microcavity polaritons," arXiv:1410.0238 (2014).
15. R. Chiao and J. Boyce, "Bogoliubov dispersion relation and the possibility of superfluidity for weakly interacting photons in a two-dimensional photon fluid," Phys. Rev. A **60**, 4114–4121 (1999).

16. Y. Pomeau and S. Rica, "Model of superflow with rotons," Phys. Rev. Lett. **71**, 247–250 (1993).
17. E. Madelung, "Quantentheorie in hydrodynamischer Form," Z. Phys. **40**, 322–326 (1927).
18. L. P. Pitaevskii and S. Stringari, *Bose-Einstein Condensation* (Clarendon, 2003).
19. J. Macher and R. Parentani, "Black-hole radiation in Bose-Einstein condensates," Phys. Rev. A **80**, 043601 (2009).
20. C. A. Carter and J. M. Harris, "Comparison of models describing the thermal lens effect," Appl. Opt. **23**, 476–481 (1984).
21. S. Sinha, A. Ray, and K. Dasgupta, "Solvent dependent nonlinear refraction in organic dye solution," J. Appl. Phys. **87**, 3222–3226 (2000).
22. W. Krolikowski, O. Bang, J. Rasmussen, and J. Wyller, "Modulational instability in nonlocal nonlinear Kerr media," Phys. Rev. E **64**, 016612 (2001).
23. A. Minovich, D. N. Neshev, A. Dreischuh, W. Krolikowski, and Y. S. Kivshar, "Experimental reconstruction of nonlocal response of thermal nonlinear optical media," Opt. Lett. **32**, 1599–1601 (2007).
24. W. Wan, S. Jia, and J. Fleischer, "Dispersive, superfluid-like shock waves in nonlinear optics," Nat. Phys. **3**, 46–51 (2007).
25. N. Ghofraniha, C. Conti, G. Ruocco, and S. Trillo, "Shocks in nonlocal media," Phys. Rev. Lett. **99**, 043903 (2007).
26. C. Barsi, W. Wan, C. Sun, and J. W. Fleischer, "Dispersive shock waves with nonlocal nonlinearity," Opt. Lett. **32**, 2930–2932 (2007).
27. S. Bar-Ad, R. Schilling, and V. Fleurov, "Nonlocality and fluctuations near the optical analog of a sonic horizon," Phys. Rev. A **87**, 013802 (2013).
28. L. Rindorf and O. Bang, "Highly sensitive refractometer with a photonic-crystal-fiber long-period grating," Opt. Lett. **33**, 563–565 (2008).
29. D. Stilwell, "Directional energy spectra of the sea from photographs," J. Geophys. Res. **74**, 1974–1986 (1969).
30. J. Dugan, H. Suzukawa, C. Forsyth, and M. Farber, "Ocean wave dispersion surface measured with airborne IR imaging system," IEEE Trans. Geosci. Remote Sens. **34**, 1282–1284 (1996).
31. S. Weinfurtner, E. W. Tedford, M. C. J. Penrice, W. G. Unruh, and G. A. Lawrence, "Measurement of stimulated Hawking emission in an analogue system," Phys. Rev. Lett. **106**, 021302 (2011).
32. C. Barsi, W. Wan, and J. W. Fleischer, "Imaging through nonlinear media using digital holography," Nat. Photonics **3**, 211–215 (2009).
33. C. Bosshard, P. V. Mamyshev, and G. I. Stegeman, "All-optical steering of dark spatial soliton arrays and the beams guided by them," Opt. Lett. **19**, 90–92 (1994).
34. P. V. Mamyshev, C. Bosshard, and G. I. Stegeman, "Generation of a periodic array of dark spatial solitons in the regime of effective amplification," J. Opt. Soc. Am. B **11**, 1254–1260 (1994).
35. N. Ghofraniha, L. S. Amato, V. Folli, S. Trillo, E. DelRe, and C. Conti, "Measurement of scaling laws for shock waves in thermal nonlocal media," Opt. Lett. **37**, 2325–2327 (2012).
36. Y. Pomeau and S. Rica, "Diffraction non linéaire," C. R. Acad. Sci. Paris **t.317**, 1287–1292 (1993).